

Spall Strength and Shock Release Kinetics Following the Alpha-Epsilon Phase Transition in Iron

L. R. Veaser (P-22) and R. S. Hixson, J. E. Vorthman, and D. B. Hayes (DX-1)

Introduction

Spall, the dynamic fracture of a material, can occur when the tensile stresses from colliding rarefaction waves* exceed the strength of the material. By passing rarefactions through a sufficiently thick sample, they can be made to rise relatively slowly to allow detection of dynamic features of the spall. We are using techniques, many of which were developed over several decades by shock-wave experts at Los Alamos and elsewhere, to study spall in iron. Iron is known to experience an alpha-to-epsilon [bcc to hcp, body-centered cubic to hexagonal close packed] phase transition, which has a significant density change, when shocked to pressures above about 13 GPa (130 kbar). This phase change was studied extensively by Barker and Hollenbach¹ and others. We are interested in spall of the material after it transforms from alpha to epsilon phase and reverts to alpha. Studies of recovered targets of similarly spalled iron indicate increased shock hardening relative to targets shocked to below the transition.² We also studied the kinetics of shock release from the epsilon state for the case where spall is suppressed by placing an impedance-matched window adjacent to the target.

Measurements

Spallation

The experiments were performed using a 50-mm-diameter light gas gun, one of several research guns owned and used by Group DX-1. The gun accelerates a flyer plate a few millimeters thick and 50 mm in diameter to speeds of up to about 800 m/s, and the flyer impacts inelastically onto a target. In this work the target and usually the flyer are iron. Strong, planar shock waves are produced at the flyer-target interface and propagate

both forward into the target and backward into the flyer plate. These shock waves reflect at the distal surfaces of both the flyer and target and travel as rarefactions back into the flyer and target. Rarefactions are pressure-reducing waves. Each of the rarefactions reduces the pressure from its peak to near zero pressure. When they collide, large tensions are produced. It is the interactions of these rarefactions that are of interest here. By suitable design of the experiment we arrange for them to collide in the target, and where they meet the tension can spall it. Figure 1 shows (upper) a schematic of a flyer and spalled target and (lower) a graph (time vs position) of the shock fronts and rarefactions. While a shock front typically

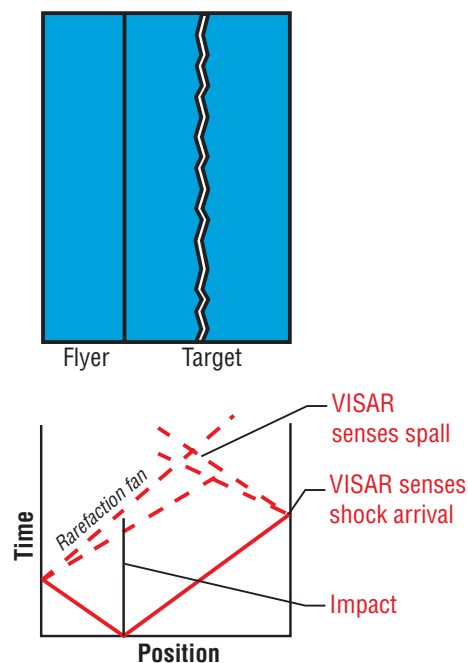


Figure 1. Upper: Schematic of a flyer in contact with a spalled target. Lower: Time vs shock positions (solid lines) and rarefaction positions (dashed lines). In this representation steeper curves imply slower waves. Spall can occur where the rarefactions collide when the tensile stresses exceed the material strength. In iron a phase change occurs, and the “shocks” are really three structures: elastic wave, plastic wave, and the phase-changing wave. The release waves have similarly complex structures.

* A pressure wave induced by the reduction in density following a shock wave; it travels in the opposite direction of the shock wave.

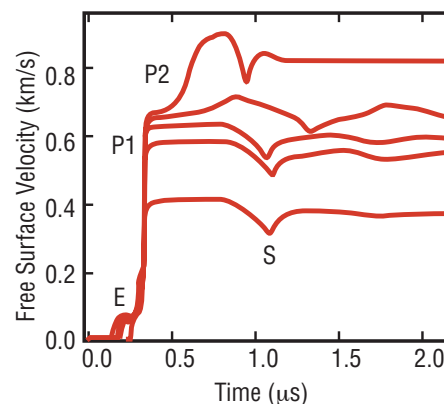
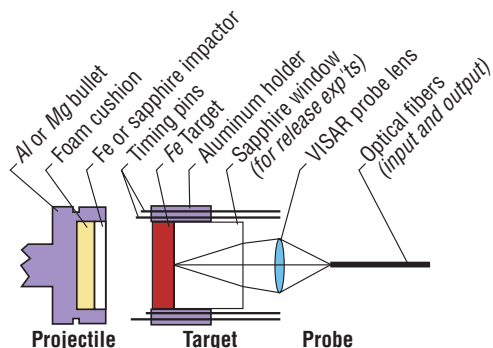
steepens as it travels through a target, a rarefaction usually spreads out with distance traveled and is better described as a rarefaction “fan.”

The free surface of the target, the surface opposite the one shocked by the gun projectile (the right boundary in Figure 1), is set into motion by the shock roughly a microsecond after impact, and it is simultaneously further accelerated by the reflection of the shock back into the target, the rarefaction. Because of the acceleration, the free-surface velocity immediately after shock release is approximately twice the particle velocity, the velocity initially given the material by the passage of the shock. (This acceleration is analogous to the doubling of an electrical pulse in reflecting from an unterminated

end of a cable.) The rarefactions, one from the release at the front surface and one from the rear surface, eventually collide near the middle of the target, and the tension is sufficient to cause the material to spall.

Figure 2 shows a schematic of the experimental set-up. It illustrates the configuration for shock-release measurements, described later. For spall there was no sapphire window in back of the iron target. The flyer, held in an aluminum or magnesium “sabot” to keep it from tilting, is accelerated in a 50-mm-diameter, single-stage, light-gas gun. A foam cushion between the flyer and the sabot allows the large rarefactions needed for these experiments to form upon shock reflection at the trailing surface of the flyer. Between six and ten electrical shorting pins, placed in a 44-mm-diameter circle around the 38-mm-diameter target, measure the flyer velocity and tilt. Flyer velocities were measured with an accuracy of $< 0.2\%$. Tilt was small, typically between 1 and 2 mrad.

Figure 2. Schematic of a shock-release experiment. For spall the set-up is similar but does not have the sapphire window in back of the iron target.



The principal diagnostic is a VISAR (Velocity Interferometer System for Any Reflector)³ measurement of the velocity of the free surface for spall or of the target-window interface for shock release. Argon-ion-laser light of wavelength 514.5 nm is brought in on an optical fiber and focused onto the target free surface. This surface is prepared by roughening it slightly to make the reflections somewhat diffuse so that the signal will not be lost if the reflecting surface tilts slightly during the experiment. The reflected light is focused into a second fiber leading back to the recording room. There the fiber-optic signal is split and sent to a pair of VISARs. By using two VISARs with different sensitivities, we can determine whether any interference fringes are lost during

Figure 3. VISAR signals for iron showing the velocity of the free surface as a function of time. Zero time was adjusted for each experiment so that the P1 waves would all arrive at the same time. In these five experiments the iron is shocked to peak pressures of (top to bottom) 16.5, 14.5, 11.0, 10.1, and 7.0 GPa. The shock wave separates into two or three distinct waves while progressing through the target, and the VISAR detects them when they arrive at the free surface and accelerate it. The first wave to appear is an elastic wave (E); it is very dependent on the microstructure of the target and therefore varies greatly from shot to shot, as various target types were investigated. Next is a plastic wave (P1), which takes the target up to a pressure no higher than that at which the alpha-to-epsilon phase transformation begins (13.0 GPa). The third wave (P2) occurs only when the shock is sufficient to cause the phase transformation; it takes the target to the final, partially-phase-transformed, state. Because the phase transformation occurs gradually, P2 rises slowly as the material transforms. Around 0.7 to 0.8 μs the leading edge of the rarefaction from the flyer arrives at the free surface, and it begins to slow. The bottom of the dip (S) indicates that the material has fractured. The depth of this dip is an indication of the spall strength. (Otherwise the free surface would have continued to slow to near zero velocity.) After spall the release of the tension allows a gap to open; the interior spalled surfaces separate and the momentum trapped in the spall slab causes ringing.

the fast-rising shock front. In these experiments typically one or two fringes are missed, and unless the proper number are added to the raw signals at shock-arrival time, the two signals will not agree. Four of the five spall tests were conducted in symmetric-impact geometry, with an iron flyer and an iron target. However to increase the pressure attainable with this gun, we used a z-cut sapphire flyer for the highest-pressure spall shot. Sapphire's large elastic modulus allows us to produce higher pressures in the iron target than using symmetric impacts at the same velocity. Both geometries were designed so that spall would occur roughly midway through the target. VISAR measurements of the free-surface velocity in five experiments are shown in Figure 3. The large dips, which occur between 0.8 and 1.3 μs in the VISAR traces, indicate the spall as shown schematically in Figure 1. The three lowest curves were for pressures below the 13-GPa phase transition. They all show a spall signal arriving at the free surface about 1 μs after the shock. The second curve from the top is for a shock at 14.5 GPa. Here the beginning of a transition to epsilon phase in the iron is

evident, but before the transition is completed the rarefaction from the flyer reduces the pressure, reverses the transition, and spalls the target. When the rarefaction from the target arrives the target spalls. These four shots had 2-mm-thick iron flyers and 4-mm-thick iron targets. The top curve was for an experiment using a 3-mm-thick sapphire flyer and a 2.2-mm-thick iron target; because this target was thinner than the others, and because the wave speed in sapphire is very fast, the spall was earlier. It is apparent from the four symmetric-impact experiments that the presence of the phase transformation above 13 GPa delays the spall considerably, suggesting an alteration in the kinetics of the damage evolution leading to spallation above and below the alpha-to-epsilon phase transition. Simulations with the hydrodynamics code⁴ WONDY indicate spall strengths of around 2.4 GPa below the transition and 3.5 GPa when the material is cycled through the phase transition and back.

Reverse phase change

To observe the reverse transformation, we conducted experiments with a thick sapphire window instead of a free surface. Laser light from the VISAR penetrated the window to view the iron. We used a 3-mm-thick, z-cut sapphire flyer, a 1-mm-thick iron target, and a 15-mm-thick, z-cut sapphire window glued to the back of the target. The sapphire's impedance (sound speed times density) is nearly that of iron, minimizing reflections at the interfaces and allowing us to observe the arrival of the rarefaction from the trailing edge of the flyer almost as it existed in the iron; *i.e.*, the shock and release pass into the sapphire largely unaffected by the window. The thin iron target guaranteed that the rarefaction from the back of the sapphire flyer did not overtake the iron shock until it had passed into the window, allowing us to observe the slowing of the target-window interface when the rarefaction arrived there. No spall occurs because one of the rarefactions has been suppressed by the presence of the window, and a single rarefaction in the iron target

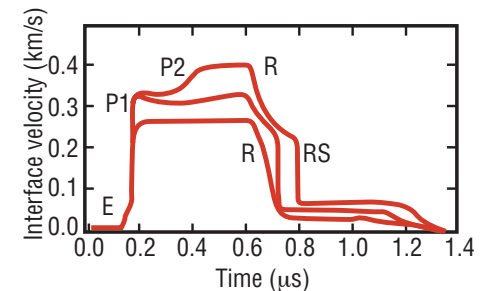


Figure 4. VISAR signals for iron, in contact with a sapphire window, showing the velocity of the target-window interface as a function of time. Zero time is arbitrary. In these three experiments the iron is shocked to pressures of (top to bottom) 16.3, 13.8, and 10.3 GPa. The shock wave separates into two or three distinct waves while progressing through the target, and the VISAR detects them when they arrive at the interface and accelerate it. The first wave to appear is an elastic wave (E). Next is a plastic wave (P1), which takes the target up in pressure no higher than that at which the alpha-to-epsilon phase transformation begins (13.0 GPa). The third wave (P2), which occurs only if the shock is sufficient to cause the phase transformation, then takes the target to the final, phase transformed, state. Because the phase transformation occurs gradually, P2 rises slowly as the material transforms. Later the leading edge of the rarefaction (R) from the flyer arrives, and the surface begins to slow. For the lowest pressure this release continues until the interface has slowed to near zero velocity. For the higher pressures the reverse phase transformation begins below 10 GPa, and it proceeds very quickly, producing a rarefaction shock (RS).

does not produce significant tensile stress. The window limited the maximum pressure in the iron to around 16 GPa; above this pressure the sapphire becomes opaque. Figure 4 shows the VISAR data for three shock-release measurements at pressures of 16.3, 13.8, and 10.3 GPa. Again, as for spall, the shock separates into an elastic wave, a P1 plastic wave, and at the higher pressures a P2 plastic wave. For the middle pressure, which is just barely above the transition, almost no P2 wave exists because the iron has just begun transforming to epsilon phase when the rarefaction arrives at the window. For the lowest curve, the 10.3 GPa shot, the rarefaction arrives at 0.6 μ s and takes the interface velocity nearly to zero in about 100 ns. For the two upper curves the rarefaction again appears at 0.6 μ s, but when the velocity has dropped to about 200 m/s a rarefaction shock forms. This shock indicates the reverse transformation, from epsilon phase back to alpha-phase iron. The density of iron in its epsilon phase is about 6% larger than in alpha phase. Upon reverse phase transformation, the density drops and the sound speed increases. The result is

a sudden steepening of the rarefaction front, a rarefaction shock. (Zel'dovich and Raizer give a good description of rarefaction shocks in Reference 5.) The slope of the rarefaction shock is steeper than can be resolved by the VISAR, implying that the reverse transition occurs in less than 1 or 2 ns, much faster than the forward transition rate. In contrast, the release in the 10.3-GPa experiment never forms a shock, indicating that there was no transformation to the epsilon phase.

Calculations

To simulate the shock experiments, we used a one-dimensional, Lagrangian, finite-difference wave propagation code⁴, WONDY, using a nonequilibrium-mixture model developed for iron by Andrews.^{6,7} The model assumes that for mixed phases of material, constituent phases locally share the same pressure and temperature but are not otherwise necessarily in equilibrium. Others have used this assumption extensively since the mid-1960s for modeling the dynamics of nonequilibrium phases. Experimental studies on numerous materials have shown that the phase-change rate is not constant but that the first part of the transformation proceeds rapidly to a metastable state and that the subsequent transformation proceeds either slowly or not at all.^{1,8} Iron displays such behavior, having a fast (tens of nanoseconds) but measurable initial rate to a metastable state with essentially no subsequent transformation until conditions are changed by various impinging waves. The metastable state is best modeled by adding a

term to the Gibbs potential of the high-pressure phase.⁹ The modified potential is

$$G_2' = G_2 - C \log(1-X_2) \quad (1)$$

where G_2' and G_2 are the Gibbs potentials for the high-pressure phase in the metastable and in the equilibrium condition, respectively; X_2 is the mass fraction of the high-pressure phase; and C is a constant determined by matching the calculations to the measurements. We used $C = 1.15 \times 10^8$ [erg/g]. This modification to the Gibbs potential has the effect of causing our calculated phase transformation to halt when the metastable state is reached. We described the kinetics of the phase change by a simple phenomenological model in which the rate of transformation is proportional to $G_1 - G_2'$, where G_1 is the Gibbs potential for alpha-phase iron. The proportionality constant was chosen to match the transformation rates in the experiments. It is likely that strength effects during phase transformations are quite complex. However, our constitutive behavior was modeled as elastic, perfectly plastic.

Figure 5 shows a comparison of the measurements with the WONDY simulations for both a spall and a shock-release measurement. The elastic wave, the small precursor to the main shock rise, is a sensitive indicator of the material purity. We measured targets of varying purity to see what effects there would be on the spall and release signals, but differences were minimal despite large differences in the elastic-wave appearance. We did not develop a detailed model of the elastic waves. The calculated rarefactions have wiggles in them from the reflections

of the elastic precursors, while in the data the rarefactions have smoothed out. Calculations of the shape and timing of the spall dip agree well when we used proportionality constants which fit the P2 rise times¹ and the P1 decays.¹⁰ For the release measurements, we have generally good agreement, but the timing of the calculated rarefaction arrival and the rarefaction shock onset do not quite exactly match the measurements. Small changes to some of the parameters will be needed. We intend to obtain more shock-release data at pressures above the transformation to better define these parameters.

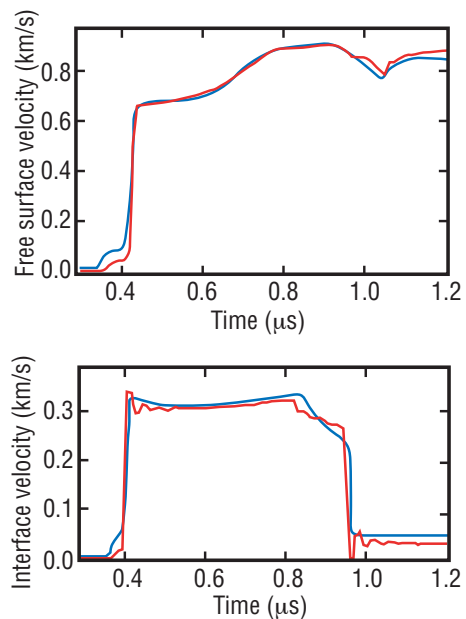


Figure 5. Comparisons of measured velocity data (blue curves) with the WONDY simulations (red curves) for iron that has transformed to the epsilon phase. The upper graph is for spall at 16.5 GPa and the lower graph is for a shock-release experiment at 13.8 GPa.

Summary

We have seen that the alpha-to-epsilon phase transformation in iron increases the spall strength by about 50%. This result is consistent with measurements of increased hardness of similarly shocked samples.² Our simulations of the phase transformation to alpha phase show that the transformation requires a few tens of nanoseconds, in agreement with previous results.¹ In our data we found that the reverse transformation, in contrast, proceeds in < 2 ns.

About the Team

Robert S. Hixson has been involved in dynamic material properties research for the last 25 years. Rob has co-authored dozens of publications in the area of shock compression of condensed matter, with some work in static high pressure physics as well as the physics of expanded liquid metal states. Rob is currently team leader of the shock physics team within group DX-1 of the Dynamic Experiments Division. The gas gun used for this experiment is one of several operated by his team. Like Hixson, John Vorthman, has been using gas guns for over 25 years. In addition to research on various metals he has used shock waves to study the dynamics of high explosives. John also spent several years working on explosive-pulsed-power devices. Dennis Hayes has a long-standing interest and research record in shock waves and phase transformations. He presently works part time at Los Alamos (DX-1), Sandia National Laboratories, and Washington State University. All three of the authors above earned Ph.D. degrees from Washington State University.

Lynn Veaser has worked on a wide variety of basic and applied physics problems in nuclear, plasma, pulsed-power, and shock-wave physics at Los Alamos for the past 33 years and has roughly 100 publications in those areas. He is the deputy group leader of Hydrodynamics and X-Ray Physics group (P-22). His Ph.D. is from the University of Wisconsin.

Acknowledgments

We are grateful to the many people who helped with these experiments. In particular Max Winkler fielded the VISAR, David Kachelmeier, Pat Rodriguez, and Mark Byers built many of the targets and flyers, Rusty Gray characterized the iron targets, and Joe Andrews provided us his iron EOS for the WONDY code. This work was performed under the auspices of the U.S. Department of Energy.

References

- ¹ L. M. Barker, R. E. Hollenbach, *J. Appl. Physics* 45, 4872–4887 (1974).
- ² G. T. Gray, D. B. Hayes, R. S. Hixson, *J. de Physique IV* 10, 755–760 (2000).
- ³ L. M. Barker, R. E. Hollenbach, *J. Appl. Physics* 43, 4669–4675 (1972).
- ⁴ M. E. Kipp, R. J. Lawrence, Sandia National Laboratories report SAND81-0930 (1982).
- ⁵ Ya. B. Zel'dovich, Yu. P. Raizer, *Physics of Shock Waves and High-Temperature Phenomena*, (Academic Press, New York, 1967) pp. 757–762.
- ⁶ D. J. Andrews, *J. Phys. Chem. Solids* 34, 825–840 (1973).
- ⁷ D. J. Andrews, *J. Comp. Phys.* 7, 310–326 (1971).
- ⁸ D. B. Hayes, *J. Appl. Phys.* 46, 3438–3443 (1975).
- ⁹ J. C. Boettger, D. C. Wallace, “Metastability and Dynamics of the Shock-Induced Phase Transition in Iron,” *Phys. Rev. B* 55, 2840–2849 (1997).
- ¹⁰ R. S. Hixson, J. E. Vorthman, private communication (1999).